TWENTY FIRST EUROPEAN ROTORCRAFT FORUM

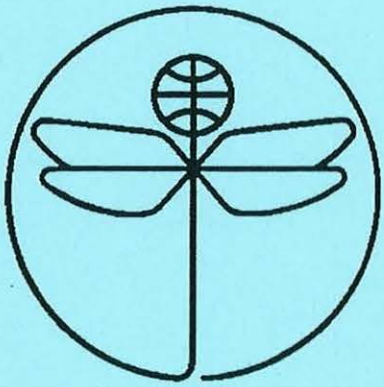

Paper No XI.2

RELIABILITY OF EDDY CURRENT INSPECTION OF THIN ALUMINUM ALLOY PLATES

BY

G. Surace, M. Villani, E. Carrera

Department Aeronautical and Space Engineering
Politecnico di Torino
ITALY

August 30 - September 1, 1995

SAINT - PETERSBURG, RUSSIA

Paper nr.: XI.2

Reliability of Eddy Current Inspections of Thin Aluminum Alloy Plates.

G. Surace; M. Villani; E. Carrera

TWENTY FIRST EUROPEAN ROTORCRAFT FORUM
August 30 - September 1, 1995 Saint-Petersburg, Russia

RELIABILITY OF EDDY CURRENT INSPECTION OF THIN ALUMINUM ALLOY PLATES

G. Surace*, M. Villani†, E. Carrera‡

Department of Aeronautical and Space Engineering
Politecnico di Torino
Corso Duca degli Abruzzi, 24, 10129 Torino, Italia

Abstract

The paper presents the major results of a research program funded by the Italian National Research Council (CNR) and conducted by the Department of Aeronautical and Space Engineering of the *Politecnico di Torino* together with the *Alenia Spazio* thermo-mechanical laboratory of *Torino*. The reliability of the Eddy Current technique in detecting EDM notches produced on thin (1.2 mm) samples of aluminum sheet was investigated. Results are presented in the form of Probability Of Detection curves and the corresponding lower 95% confidence limits.

1 Introduction

Major portions of the structures of aerospace, helicopter, automotive and marine vehicles consist of flat and curved panels that are used as primary load carrying components. Hence there are a number of situations of technological importance in which it is advisable to carry out Nondestructive Inspection (NDI) of these structures. Eddy Current (EC) applications in the aerospace and helicopter industries differ from those found in the automotive and semi-finished products industries. The primary difference is that aerospace and helicopter EC tests are maintenance rather than production oriented. Maintenance inspections usually deal with the inspection of parts and components that are already in service. Examples include the inspection of critical areas on an aircraft or helicopter, such as engine parts or main structural components. Safety is obviously a primary issue in maintenance inspections. As a matter of fact, materials are not perfect structures and hence below any set level of inspection, components contain structural irregularities and defects. Any viable lifing methodology must directly or indirectly address the effects of these defects on component life. The various approaches to component lifing include Safe Life, Damage Tolerance and Retirement For Cause (RFC) procedures (Ref 1).

For many years, the Safe Life methodology has been the basis of lifing procedures (Predicted Safe Cyclic Life, PSCL). In this approach, parts are designed for a finite

*Professor
†Doctoral Student
‡Research Engineer

service life during which it is assumed that no significant damage will occur. No in-service inspection is necessary and safety is ensured by requiring components to be withdrawn from service before any detectable cracks have appeared.

In Damage Tolerance approaches to component lifing, damage is assumed to exist in the newly manufactured component. This damage is considered to take the form of small defects in the material whose size is generally set by the minimum level detectable by the NDI system used in final inspection. Again, the residual life of the component is then determined by applying fracture mechanics concepts to calculate the cycles required to grow this maximum initial defect to a critical size (Ref 2-5). To assess the reliability of such procedures, it is necessary to construct Probability Of Detection (POD) curves for the NDI system used. This requires a representative set of component test specimens for inspection and application of appropriate statistical procedures to analyze and correlate the results.

In RFC, retirement is not implemented until cracks have been identified in individual components. RFC uses in-service inspections to declare iterative life extensions beyond the damage tolerant life. As service lives are extended beyond the PSCL, and hence as more components will be cracked at each inspection interval, the reliability of the NDI system must be increased in order to maintain the original safety levels. In practice, this can really only be achieved by increasing the detectable crack size, i.e. by setting larger size NDI limits.

The importance of the role played by NDI techniques in this connection is clear. Recently, in fact, it has been found necessary to refine fracture mechanics design concepts in order to make better use of materials and reduce structural masses. This entails refining and developing NDI methods and procedures capable of detecting flaws whose initial dimensions are smaller than the standards hitherto used in establishing reliability requirements based on the Fitness for Purpose concept. The benefits to be gained from such an approach are enormous. The aerospace and helicopter industries, for instance, can improve market competitiveness in terms of increased structural performance with lower masses, and thus lower manufacturing and operating costs, with no loss of safety.

In this context, the paper presents the procedures and major results of an investigation of the reliability of the EC technique in detecting defects in 1.2 mm thick samples of Al 2219-T851. The purpose of the investigation was to quantify the capacities of this technique by evaluating the minimum flaw size which can be detected with 90% probability and 95% confidence compatibly with the flaw sizes dictated by the limited sample thickness.

2 Stochastic models for assessing the reliability of flawed structures

NDI systems are essentially probabilistic in nature (Ref 6,7). For this reason, the ability to detect flaws is expressed in terms of POD(a), where a is a characteristic flaw size. The function in question can reasonably be modelled by the cumulative log-normal distribution function or, equivalently, by the log-log function. The parameters of these functions can be estimated using Maximum Likelihood methods. In addition, the statistical uncertainty of the reliability estimate is conventionally expressed by a confidence limit for the POD(a) function.

There are two ways to carry out a statistical analysis of experimental reliability data. The first is based on Hit/Miss data, i.e. on establishing whether or not a flaw is detected. The second is based on the correlation between the characteristic flaw size and the strength of the response signal for the NDI technique used.

Hit/Miss analysis

This analysis originates from a binomial approach. The POD(a) function is defined as the fraction of all flaws which will be identified with a particular NDI system. It is assumed that each flaw of size a in a potential flaw population has its own probability of detection, p. The probability density function for detection probabilities is given by $f_a(p)$. Thus, the POD(a) function can be expressed as:

$$POD(a) = \int_0^1 p\, f_a(p)\, dp \tag{1}$$

i.e. as the average of the probabilities of detection for flaws of size a.

The following three mathematical forms can be derived:

$$POD(a) = \frac{\exp(\alpha + \beta \ln a)}{1 + \exp(\alpha + \beta \ln a)} \tag{2}$$

$$\ln\left[\frac{POD(a)}{1 - POD(a)}\right] = \alpha + \beta \ln a \tag{3}$$

$$POD(a) = \left\{1 + \exp\left[-\frac{\pi}{\sqrt{3}}\left(\frac{\ln a - \mu}{\sigma}\right)\right]\right\}^{-1} \tag{4}$$

In the latter expression, $\mu = \ln a_{0.5}$, where $a_{0.5}$ is the size of the flaw having POD(a) = 0.5. The parameters of the three mathematical forms shown are correlated as follows:

$$\mu = -\frac{\alpha}{\beta} \qquad \sigma = \frac{\pi}{\beta\sqrt{3}} \tag{5}$$

and are determined using the Maximum Likelihood model. α and β are not readily interpreted in physical terms (Ref 6).

â–a analysis

The indications of a nondestructive evaluation system are based on interpreting the response to a stimulus applied to the object under test. With EC or ultrasonic inspection methods, the response may be obtained in volts, relative to a certain system calibration. It is assumed that this response, $\hat{a}$, can be quantified and correlated to flaw size a. Thus, $\hat{a}$ contains the information which makes it possible to establish whether or not a certain indication reveals the presence of a flaw. Only if $\hat{a}$ exceeds a predetermined decision threshold $\hat{a}_{dec}$ can it be assumed that the indication is due to the presence of a flaw. In this case, the POD(a) function can be defined starting from the relation between $\hat{a}$ and a. If $g_a(\hat{a})$ is the probability density of the values of $\hat{a}$ for a given flaw size a, then:

$$POD(a) = \int_{\hat{a}_{dec}}^{\infty} g_a(\hat{a})\, d\hat{a} \tag{6}$$

Analysis of data of this kind shows that there is a linearity relation:

$$\ln \hat{a} = \beta_0 + \beta_1 \ln a + \delta \tag{7}$$

where δ is a random error with normal distribution, zero mean and constant standard deviation σ_δ . β_0 and β_1 are the intersection with the vertical axis and the slope of the line respectively. This relation is valid for a fairly small range of flaws (Ref 6). With these assumptions, a mathematical expression can be formulated for the POD(a) function. Noting that POD(a) = *probability*[$\ln \hat{a} > \ln \hat{a}_{dec}$] and introducing the standard normal distribution $\Phi(z)$ allows us to write:

$$POD(a) = \Phi \left\{ \frac{\ln a - \frac{[\ln \hat{a}_{dec} - \beta_0]}{\beta_1}}{\frac{\sigma_\delta}{\beta_1}} \right\} \tag{8}$$

This equation is a cumulative log-normal distribution, with mean and standard deviation of $\ln a$ given by $\mu = \frac{\ln \hat{a}_{dec} - \beta_0}{\beta_1}$ and $\sigma = \frac{\sigma_\delta}{\beta_1}$.

Maximum Likelihood analysis

A common statistical technique for estimating the POD(a) parameters is based on the Maximum Likelihood method. This technique describes the parameters' behaviour once data have been established. Let X_i be the result of the i–nth inspection and $f(X_i, \Theta)$ the probability that this result is found, where $\Theta = (\theta_1, \ldots, \theta_k)$ is the vector of the parameters for the probabilistic model used. In Hit/Miss analysis, X_i can be 0 or 1, with a probability defined by (4), where a is the size of the i-nth flaw. In $\hat{a}$–a analysis, on the other hand, X_i is the logarithm of the response signal. The likelihood function is given by:

$$L(\Theta) = \prod_{i=1}^{i=n} f(X_i, \Theta) \tag{9}$$

where n is the number of flaws inspected. The Maximum Likelihood estimate for the parameters of the statistical model used, $\tilde{\Theta}$, is the value of Θ for which the function (9) is maximum. For the models considered, it is advantageous to work with the logarithm of this function, i.e.:

$$\log(L(\Theta)) = \sum_{i=1}^{i=n} \log[f(X_i, \Theta)] \tag{10}$$

which is still maximum for $\Theta = \tilde{\Theta}$. The Maximum Likelihood estimates are given by the simultaneous solutions of the k equations :

$$\frac{\partial \log L(\Theta)}{\partial \theta_j} = 0 \qquad j = 0, 1, \ldots, k \tag{11}$$

Discussion

In a Hit/Miss analysis, it can be assumed that flaws corresponding to $\hat{a}$ signals below $\hat{a}_{dec}$ are not detected, while large flaws provide little information for the POD(a) curve. It is thus understandable that the effective sample size is often smaller than the total number

of flaws. The range of useful flaw sizes is not known beforehand, nor can a set of test pieces be fabricated ad hoc for a given experiment. Consequently, the best solution is to distribute flaw sizes uniformly between a minimum and a maximum of potential interest.

In an $\hat{a}$–a analysis, all values bring the maximum information to the relationship between signal and flaw size. Thanks to this greater wealth of information, a minimum of around 30 flaws is sufficient.

3 Definition of a first set of sample flaws

A first set of sample flaws was produced in order to provide information concerning the possibility of obtaining valid results. The operations followed in producing these samples are described below.

Sample flaws

Geometry and dimensions were defined for eight different semi-elliptical notches as indicated below. Notch depth (a) was established on the basis of percentages of test piece thickness (t) equal to 20, 40, 60 and 80% t, while two ratios $\frac{a}{2c} = 0.1, 0.5$ were used, where c is half the notch length. As regards notch width, it is necessary that the latter be the minimum compatible with the technique used to produce these flaws in order to come as close as possible to the configuration of real cracks, where thickness is practically zero.

Test pieces

The material used was available in the form of plates measuring 1000 × 150 × 2.5 mm. Thirty-one test pieces measuring 100 × 75 × 2.5 mm were cut from two plates using a shearing machine. Flaws were produced in 11 of these 31 test pieces, while the remaining 20 were used in an unflawed condition as envisaged by the applicable standards, and mixed with the flawed test pieces in order to guarantee a certain randomness during inspection. As test piece thickness was 2.5 mm (the material in question is not produced in 1.2 mm thick plates (Ref 8)), it was necessary to machine down each test piece to the desired 1.2 mm thickness. This operation was performed at a precision machine shop, which also produced the sample flaws. Test pieces were machined to a surface roughness of $Ra = 0.4 \div 0.5\,\mu m$.

Flawed test pieces

Once the test pieces had been machined down to the desired thickness, flaws as described in section 3.1 were produced through Electrical Discharge Machining (EDM), as envisaged by the standards. Test requirements called for a total of twelve notches. Because of the limitations imposed by electrode dimensions, it was not possible to achieve a notch width of less than 0.1 mm. Two notches were produced in each test piece; in some cases a notch was produced on both sides of the piece. In addition, notches were placed so that there were no flaws adjacent to the edges of the test pieces, where detection problems would have occurred because of the edge effect (Ref 9).

Notches with the desired semi-elliptical shape could not be produced because of electrode wear. In particular, the contour located at the maximum distance from the test specimen surface was flattened. As this limitation made it impossible to respect both dimensional requirements (length 2 c and depth a), it was decided to respect only the depth requirement.

Flaw size check

Flaws were measured to check that their actual dimensions were as required, and to establish a certain correspondence between the EC signal and flaw size. Prior to this check, all flawed test pieces were cleaned ultrasonically in a solution containing isopropyl alcohol and acetone to eliminate any impurities in the flaws which could lead to incorrect readings. Dimensional checks were carried out using a stereoscopic optical microscope, ceramic specimen blocks, a comparator and a fiber optic system for illuminating the flaws in depth. The geometric features located on the test piece surface could be measured immediately using the microscope's graduated scale. For flaw depth measurements, on the other hand, it was necessary to calibrate the microscope in order to correlate the focus and hence the displacement of the optical system to flaw depth. The procedure used (Ref 10) made it possible to avoid destructive techniques which would have inevitably jeopardized the ability to use the test pieces for further assessments. Measurement results were expressed as the average of five readings for each characteristic dimension and each flaw.

4 Definition of an additional set of sample flaws

One of the basic conditions for achieving valid results from a statistical analysis of NDI reliability is to have a sufficiently large sample of flaws. As examination of the results for the first set of sample flaws indicated that the levels of the POD curves and the corresponding lower confidence limits were too low for useful conclusions to be drawn, and considering the fact that these results were not entirely discouraging, a further set of sample flaws was prepared. In particular, a further 15 notches were produced on a total of 8 new test pieces. Flaw dimensions were limited to the range which preliminary checks had shown to be most critical, i.e., that of small flaws. Here again, the procedures described above were used.

The total available sample thus consisted of 27 notches (16 flawed test pieces and 20 flaw-free pieces). Notch geometry and an example of their placement on one of the test pieces is shown in Figure 1, while Table 1 shows the characteristics of the total sample of notches. Volume was calculated regarding the notch as a semi-ellipse, without considering the slight flattening at the bottom of the notch caused by electrode wear.

5 EC Equipment

In view of the characteristics of the test pieces and of their limited thickness in particular, the EC technique was used for flaw detection (Ref 9). Inspection was carried out both manually and semi-automatically, adapting the probes to the movement system of the ultrasonic test instrumentation available at the laboratory. The instrument is a Tecrad

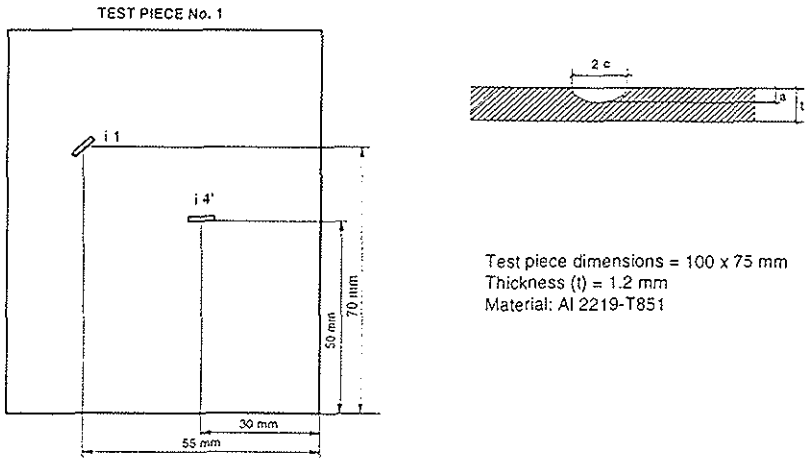

Figure 1: Notch geometry and example of placement on test pieces

TC 1100 unit capable of operating in a frequency range of 100 Hz to 6 MHz in order to characterize the probe and determine the optimum inspection frequency.

		Nominal dimensions				Effective dimensions				
Test piece	Notch	a	2 c	b	a/2c	a	2 c	b	a/2c	Volume
		mm	mm	mm		mm	mm	mm		mm^3
First set of sample notches										
1	i1	0.96	9.60	0.1	0.1	0.96	10.4	0.14	0.092	1.098
3	i2	0.72	7.20	0.1	0.1	0.69	8.56	0.13	0.081	0.603
2	i3	0.48	4.80	0.1	0.1	0.46	5.40	0.12	0.085	0.234
1	i4'	0.24	2.40	0.1	0.1	0.25	2.78	0.17	0.090	0.093
5	i4"	0.24	2.40	0.1	0.1	0.23	3.00	0.15	0.077	0.081
2	i5	0.96	1.92	0.1	0.5	0.94	2.12	0.12	0.443	0.196
4	i6'	0.72	1.44	0.1	0.5	0.75	1.65	0.14	0.454	0.136
7	i6"	0.72	1.44	0.1	0.5	0.72	1.70	0.14	0.423	0.134
4	i7'	0.48	0.96	0.1	0.5	0.47	0.96	0.11	0.489	0.039
6	i7"	0.48	0.96	0.1	0.5	0.49	1.20	0.12	0.408	0.055
3	i8'	0.24	0.48	0.1	0.5	0.26	0.57	0.10	0.456	0.012
8	i8"	0.24	0.48	0.1	0.5	0.22	0.58	0.11	0.379	0.011
Second set of sample notches										
12	i9	0.36	1.92	0.1	0.187	0.28	2.26	0.11	0.124	0.055
17	i10	0.24	1.92	0.1	0.125	0.20	2.34	0.10	0.085	0.037
14	i11	0.48	1.68	0.1	0.286	0.44	2.00	0.14	0.220	0.097
13	i12	0.24	1.68	0.1	0.143	0.21	1.90	0.11	0.110	0.034
18	i13	0.48	1.44	0.1	0.333	0.47	1.63	0.11	0.288	0.067
18	i14	0.36	1.44	0.1	0.250	0.36	1.68	0.14	0.214	0.066
15	i15	0.24	1.44	0.1	0.167	0.21	1.86	0.19	0.113	0.058
17	i16	0.60	1.20	0.1	0.500	0.57	1.30	0.13	0.438	0.076
14	i17	0.48	1.20	0.1	0.400	0.44	1.29	0.11	0.341	0.049
16	i18	0.36	1.20	0.1	0.300	0.37	1.44	0.11	0.257	0.046
19	i19	0.24	1.20	0.1	0.200	0.23	1.49	0.11	0.154	0.030
15	i20	0.36	0.96	0.1	0.375	0.36	1.10	0.11	0.327	0.034
12	i21	0.24	0.96	0.1	0.250	0.23	1.16	0.11	0.198	0.023
16	i22	0.36	0.72	0.1	0.500	0.35	0.73	0.10	0.479	0.020
13	i23	0.24	0.72	0.1	0.333	0.25	1.01	0.11	0.247	0.022

Table 1: Notch characteristics. a = depth; 2c = length; b = width

In addition, the instrument is capable of both absolute and differential measurements. Available instrumentation was completed through the addition of three probes designed especially for the operating conditions described above and produced by the same company which machined the sample flaws. Probe characteristics are shown in Figure 2. Probes consist of a casing, an internal spring, a 1.65 mm diameter ferrite core and

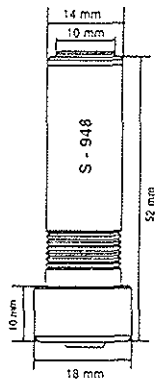

Probe	Code	Frequency
1	S - 949	1 kHz - 10 kHz
2	S - 948	5 kHz - 100 kHz
3	S - 947	100 kHz - 1 MHz

Ferrite core: ø 1.65 x 14.2 mm

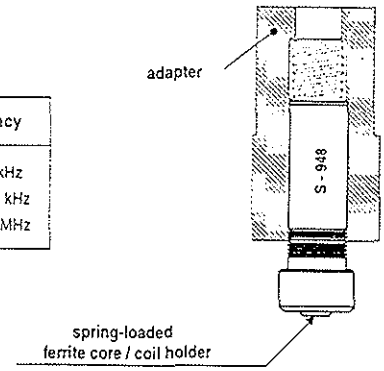

Figure 2: Probe characteristics.

a cable. Electrical connection is absolute differential, as the test coil features absolute configuration while interface with the instrument is achieved by connecting the test coil at one input and the reference coil, which is also contained in the casing, to the other input (differential type).

6 Results

Inspection results are indicated below. Automatic inspection was carried out first in order to eliminate the "operator" variable and thus identify the optimum conditions for the subsequent manual inspection operations. Automatic inspection followed a Hit/Miss analysis procedure, while $\hat{a}$–a analysis was used for manual inspection. Results are presented in the form of POD(a) curves (heavy line) plotted versus notch volume; the 95% lower confidence limit is also shown (light line). Similar curves can be obtained for all of the dimensions characterizing the flaw.

Automated Hit/Miss inspection

All three probes were used for this analysis. A number of preliminary operations were carried out in order to identify the optimum values of the parameters and variables involved in this type of inspection. First, the instrument/probe system was calibrated so as to have maximum response and a signal-to-noise ratio of at least three to one. This operation indicated that optimum operating frequencies for probes 1, 2 and 3 were 10, 10 and 400 kHz respectively. After scanning the test pieces several times with steps Δ between 0.2 mm and 1 mm, it was decided to use steps $\Delta_1 = 0.3$ mm and $\Delta_2 = 0.6$ mm. A scanning rate 20 mm/s was chosen. Each test was identified with a three-digit number. The first digit indicates the probe used, as shown in Figure 2. The second digit indicates the side on which scanning was performed ($1 \rightsquigarrow$ scanning from flaw side; $2 \rightsquigarrow$ scanning from side opposite flaw). Finally, the third digit indicates the scanning step ($1 \rightsquigarrow \Delta_1$; $2 \rightsquigarrow \Delta_2$). Analysis results are given in Figure 3.

The curves shown are those relating to tests which provided results of a certain interest. In particular, test 222 gave the same reliability levels as test 212. Tests 121 and 122 also gave the same results, which were, however, of little interest. Tests 111 and 211 were those which provided the best results. Probe 1 can only be used in cases where

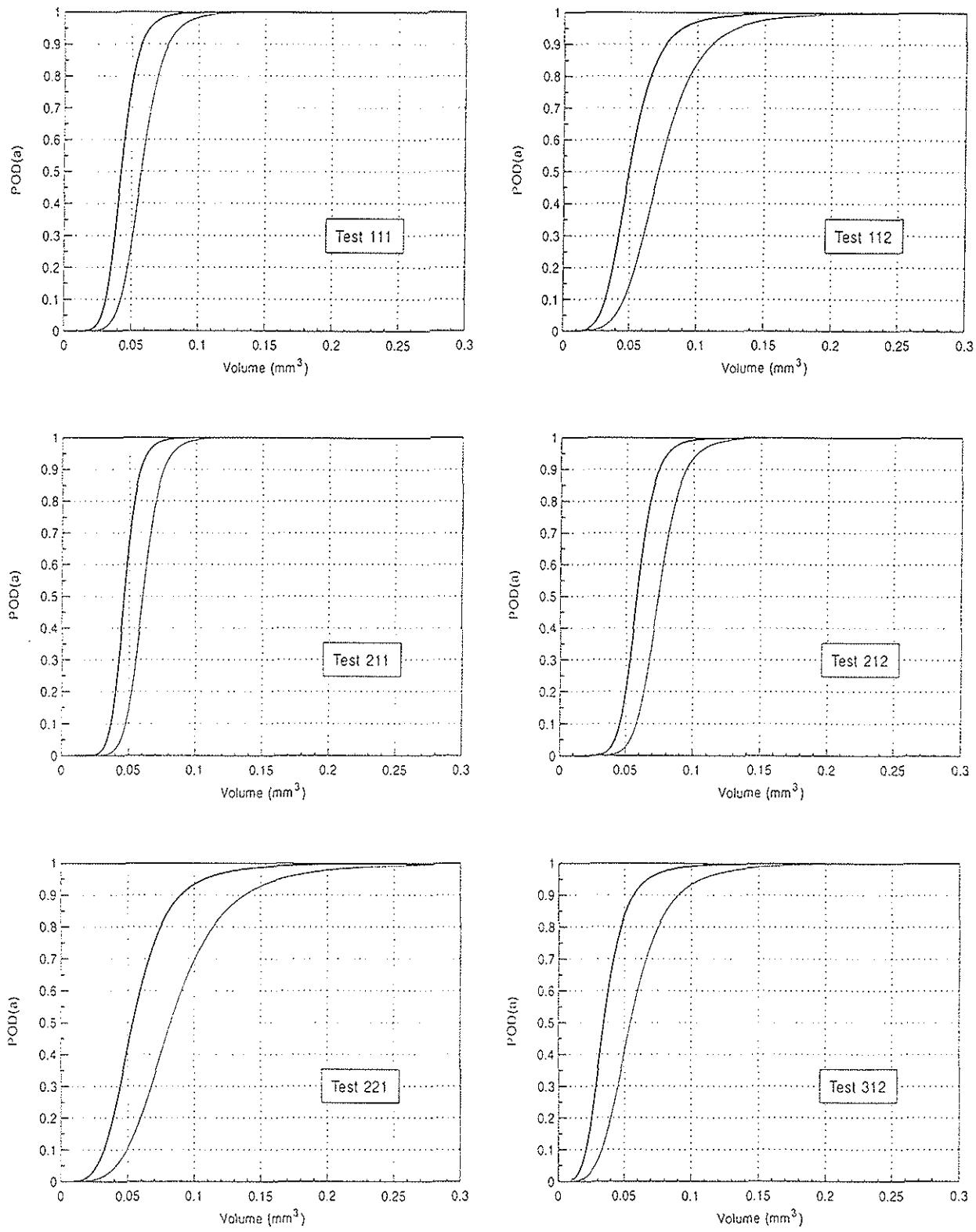

Figure 3: Results of automatic inspection. Hit/Miss analysis

scanning is performed on the flaw surface with a specific scanning step, while probe 2 can be used over a wider operating range.

Manual â–a inspection

On the basis of automatic inspection results, probe 2 was used for this analysis. Inspection was performed by specially trained operators. In this case, each test was identified with a two-digit number. The first digit indicates the inspector who performed the test, while the second indicates the side of the test piece on which scanning was carried out ($1 \rightsquigarrow$ scanning from flaw side; $2 \rightsquigarrow$ scanning from side opposite flaw). The results, which are shown in Figure 4, indicate that the curves in this case are distinctly better than those for the automatic tests. Obviously, this comparison applies to the different procedures used to analyse statistical data. In other words, as indicated in section 2, $\hat{a}$–a analyses make it possible to obtain maximum information from the response signal, rather than simply indicating whether the flaw was "Hit" or "Missed".

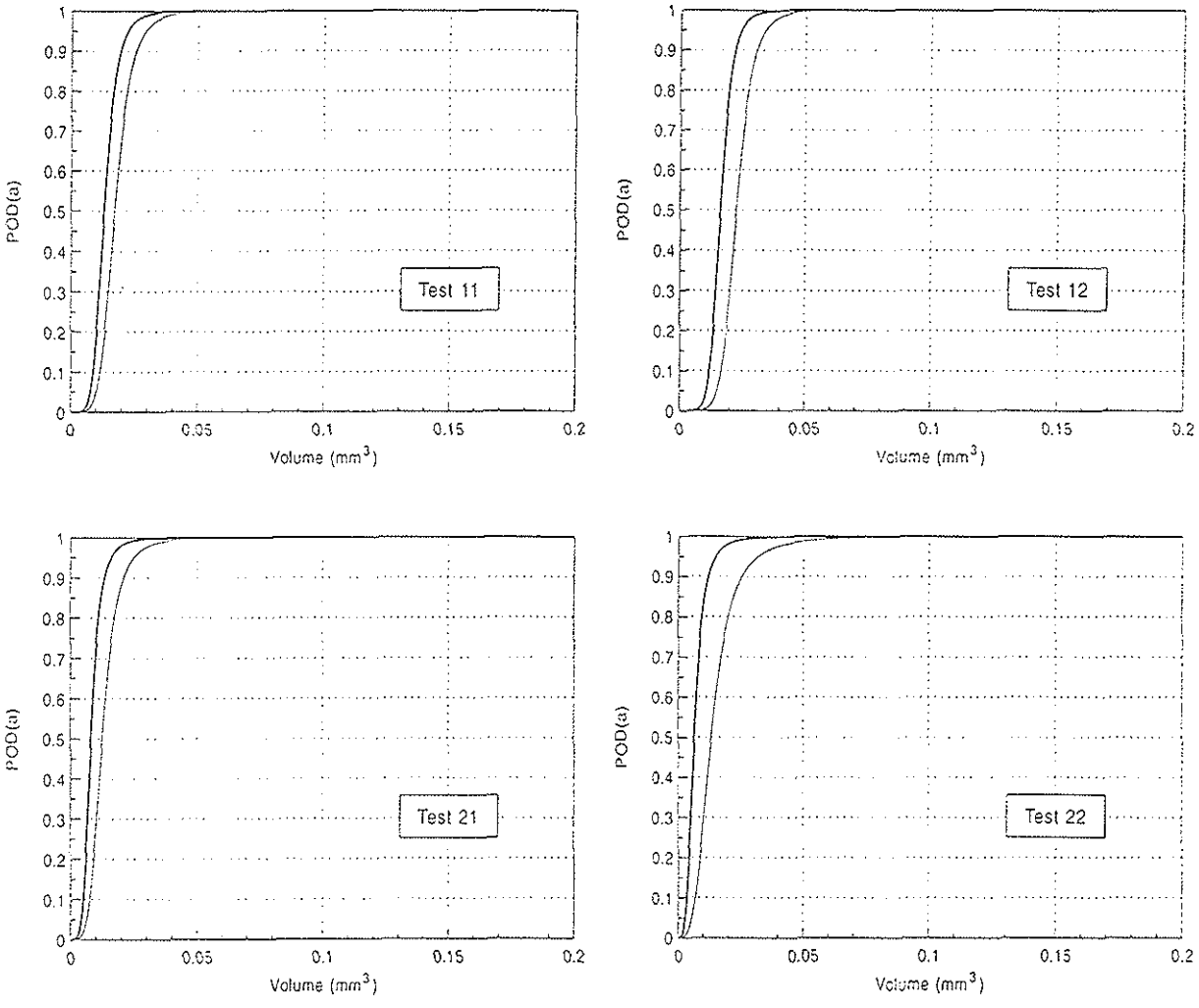

Figure 4: Results of manual inspection. $\hat{a}$–a analysis

In the end, Figure 5 presents the linear relationship between $\ln \hat{a}$ and $\ln a$ as ex-

pressed in Equation (7). The values $\hat{a}_{th}$ and $\hat{a}_{sat}$ are the recording signal threshold and the saturation limit of the recording system, respectively (Ref 6,7). In this case $\hat{a}_{th} = \hat{a}_{dec}$.

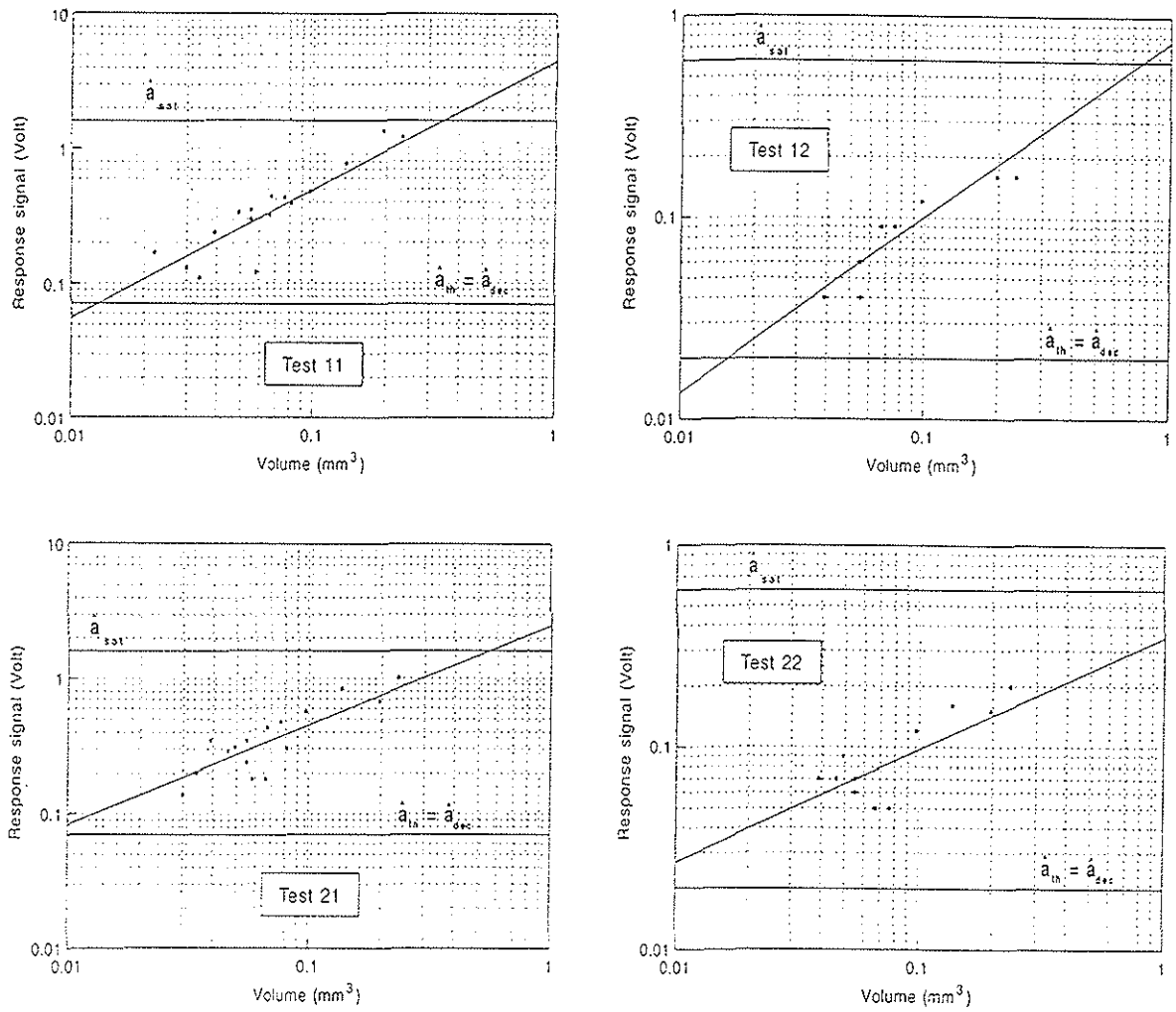

Figure 5: Manual inspection. Linear relationship between $\ln \hat{a}$ and $\ln a$.

7 Conclusions

An evaluation of the reliability of EC inspection on thin aluminum samples was presented. The results of this evaluation lead to the following conclusions.

1) In the flaw detection stage, it is necessary to allow for the limitations due to the use of notches to simulate cracks. Because of their width and regular contours, notch behaviour with regard to eddy currents is not the same as that of cracks, which have practically zero width and irregular contours.

2) Where possible, inspection should be automated and $\hat{a}$–a analysis should be used for results.

3) Using low operating frequency probes makes it possible to achieve good levels of reliability in detecting small flaws in thin components.

As regards item 1), further work is being carried out to determine whether actual cracks of known dimensions can be propagated through fatigue from surface notches produced by EDM.

8 Acknowledgements

The research described in this paper was funded by the Italian National Research Council (CNR), to which the authors wish to express their especial thanks.
Work was furthered by the fruitful cooperation with the *Alenia Spazio* thermo-mechanical laboratory in *Torino*, cooperation which was made possible through the efforts and assistance of a large number of researchers and technicians. In addition to those who were part of the research unit, the authors would like to thank the laboratory director Dr. Armando Belmondo, the technician Mr. Fernando Giuggioli, and the NDI technician Mr. Angelo Camassa.

References

1. Impact of material defects on engine structures integrity. AGARD-R-790, May 1992.
2. ESA Fracture Control Requirements. ESA PSS-01-401, March 1989.
3. Fracture Control Program Requirements, NASA MSFC-HDBK-1453.
4. Standard NDE Guidelines and Requirements for Fracture Control Programs. NASA MSFC-STD-1249, September 1985.
5. Fracture Control of Metallic Pressure Vessels. NASA SP-8040, May 1970.
6. Nondestructive Evaluation and Quality Control. Metals Handbook, Ninth Edition, American Society for Metals, Vol. 17, 1989.
7. A Recommended Methodology for Quantifying NDE/NDI Based on Aircraft Engine Experience. AGARD-LS-190, April 1993.
8. Aluminum alloy 2219, plate and sheet. Federal Specification, QQ-A-250/30A, Notice 1, 5 November 1991.
9. Electromagnetic Testing. Nondestructive Testing Handbook, Second Edition, American Society for Nondestructive Testing, Volume Four, 1986.
10. G. Surace, E. Carrera, M. Villani, Development and verification of NDI procedures for pressurized thin-wall structures for aerospace applications (in italian). DIASP, Politecnico di Torino, 1994.